NONLINEAR PHENOMENA IN COMPUTATIONAL TRANSONIC AEROELASTICITY

Elizangela Camilo
elcamilo@sc.usp.br

Flávio Donizeti Marques
fmarques@sc.usp.br
University of São Paulo - Engineering School of São Carlos
EESC/USP 13566-590 - São Carlos - SP, Brazil

João Luis Filgueiras Azevedo
azevedo@iae.cta.br
Aerospace Technical Center, Aeronautics and Space Institute
CTA/IAE/ASE-N 12228-904 - São José dos Campos - SP, Brazil

Abstract. *The study of nonlinear aeroelastic phenomena has recently received more substantial and concentrated efforts, mainly due to: (i) the advance of improved modelling methods for nonlinear phenomena; (ii) availability of efficient computational tools; and (iii) the important role played by nonlinearities in many physical problems. Transonic flow flutter and limit cycle oscillations (LCO) are of significant interest in modern wing and aircraft design. The computational fluid dynamics (CFD) has been introduced as a tools for aerodynamic research and design. As CFD and computer technology progress, higher-order methods based on the Euler equations become more attractive, because they are able to model transonic effects with more accuracy. With the maturity of recent CFD codes, their incorporation into aeroelastic analyses, for both static and dynamic, can be observed. This relatively new field has been denominated computational aeroelasticity and it involves coupling together structural and computational fluid dynamics models. There are several physical sources of nonlinearity in either the aerodynamic flow or elastic structure. In transonic flow regime the aerodynamic loads are a nonlinear function of the elastic deformation of the aircraft structure. The purpose of this work is to present results on effects of nonlinear aeroelastic response behavior in transonic regime with linear structural dynamics. A CFD code has been based on an unsteady finite volume algorithm for solving the nonlinear Euler equations. To solve the aeroelastic problem the Runge-Kutta method is applied combined with the CFD code. The aeroelastic responses are analysed by investigating typical nonlinear effects LCO from phase plane.*

Keywords: *nonlinear aeroelasticity, CFD methods, Euler equations, transonic flows, LCO.*

1. Introduction

In the last decades, nonlinear dynamics analysis has been largely developed and explored, both in the theorical and experimental point view, in a vast diversity of fields in sience and engineering. Nonlinear aeroelasticity is a mulidisciplinary field, that is very important in aeronautics and aerospace engineering (Dowell et al., 2003). Most aeroelastic analyses of flight vehicles have been performed under the assumption of linearity. Under this assumption, the characteristics of flutter and divergence can be easily obtained. However, the influence of nonlinearities on modern aircraft is becoming increasingly important and the requirement for more accurate predictive tools grows stronger (Lee et al., 1999).

There are two possible consequences of any nonlinear effect. One is that exponentially growing oscillations predicted by an unstable linear model are attenuated due to the nonlinear effects, finite amplitude, steady-state oscillation. Limit cycle oscillations (LCOs) have been a persistent problem on several fighter aircraft designs and wind-tunnel models, where it can be generally encountered on external store configurations. Bunton (2000) discusses LCO instabilities experienced during F-16 and F-18 aircraft flight tests. Denegri (2000) further elaborates extensive LCO experiences of the F-16 aircraft with external stores. LCO may be beneficial because the nonlinearity reduces the amplitude of the oscillations. Of course, structural integrity may still be an issue if the LCO amplitudes are too large. The second consequence is wholly detrimental. In this instance, a system that may be stable to a sufficiently small perturbation, can become unstable due to a large disturbance (Dowel and Tang, 2002).

LCO in aeroelastic systems appear to be more prevalent in transonic flow than in subsonic flow. Aerodynamic nonlinearity is associated with the presence of shock waves in transonic flows. The flow is assumed to be inviscid and separation does not occur. In this situation, the unsteady forces generated by motion of the shock wave have been shown to destabilize single degree-of-freedom airfoil pitching motion and affect the bending-torsional flutter by lowering the flutter speed at the so called transonic dip regime. Of course, nonlinear structural mechanisms can also lead to LCO whether the flow is transonic or not. There have designed to exhibit LCO due to a structural nonlinearity, and such test results have been successfully correlated with analysis. However, the present undertanding of LCO induced by aerodynamic nonlineari-

ties is less complete, and as yet no systematic quantitative correlation between theory and experiment has bees achieved (Thomas et al., 2002).

Computational aeroelasticity is a relatively new field emphatisizing those types of aeroelastic problems where loads based on Computational Fluid Dynamics (CFD) which can be both unsteady and nonlinear, are used to obtain solutions. A significant amount of effort devoted towards the numerical solution of transonic aeroelastic phenomena, not only in the prediction of transonic dip effects but also towards that of LCO. Euler and Navier-Stokes schemes have been coupled with structural models (Alonso, 1994; Kousen and Bendiksen, 1994; Liu et al., 2001; Kholodar et al., 2003). Several works have been directed towards the consequences of dealing with two separate meshes, one for the fluid field and the other structural. These approaches are a major advance compared to the linear doublet or vortex lattice types of approach that is still widely used throughout industry and enable nonlinear aerodynamic effects to be modelled (Cooper, 2003).

The purpose of this work is to present preliminary results on effects of nonlinear aeroelastic response behavior in transonic regime with linear structural. A CFD code has been based on an unsteady finite volume algorithm for solving the nonlinear Euler equations (Oliveira, 1993). To solve the aeroelastic problem the Runge-Kutta method is applied combined with the CFD code. The aeroelastic responses are analysed by investigating typical nonlinear effects from LCO behavior and subsequent phase plane.

2. EULER SOLUTION ALGORITHM

In the present study, the flow was assumed to be governed by the two-dimensional, time-dependent Euler equations, which may be writen in integral form for Cartesian coordinates as:

$$\frac{\partial}{\partial t}\int\int_{\mathbf{V}} \mathbf{Q}dxdy + \int_{\mathbf{S}} (\mathbf{E}dy - \mathbf{F}dx) = 0, \tag{1}$$

where $\mathbf{V}$ represents the area of the control volume and $\mathbf{S}$ is its boundary, $\mathbf{Q}$ is the vector of conserved quantities and the inviscid flux vectors, $\mathbf{E}$ and $\mathbf{F}$, are given by:

$$\mathbf{Q} = \begin{bmatrix} \rho \\ \rho u \\ \rho v \\ e \end{bmatrix}, \qquad \mathbf{E} = \begin{bmatrix} \rho U \\ \rho u U + p \\ \rho v U \\ (e+p)U + x_t p \end{bmatrix}, \qquad \mathbf{F} = \begin{bmatrix} \rho V \\ \rho V u \\ \rho V v + p \\ (e+p)V + y_t p \end{bmatrix}. \tag{2}$$

The contravariant velocity components are defined as:

$$U = u - x_t, \qquad V = v - y_t, \tag{3}$$

where x_t and y_t represents the Cartesian velocity components of the mesh.

Pressure is represented by the following state equation:

$$p = (\gamma - 1)[e - \frac{1}{2}\rho(u^2 + v^2)] \tag{4}$$

where γ is the ratio of specific heats.

The Euler equations can be rewritten for each *i-th* control volume as:

$$\frac{\partial}{\partial t}(V_i \mathbf{Q}_i) + \int_{S_i} (\mathbf{E}dy - \mathbf{F}dx) = 0. \tag{5}$$

The Euler equations are a set of nondissipative hyperbolic conservation laws. Hence, their numerical solution requires the introdution of artificial dissipation terms in order to avoid oscillations near shock waves and to damp high frequency uncoupled error modes. In Jameson et al. (1981) the numerical dissipation terms are formed as a careful blend of undivided Laplacian and biharmonic operators. Hence, the artificial dissipation operator, D_i, can be written as,

$$D_i = d^2(\mathbf{Q}_i) - d^4(\mathbf{Q}_i), \tag{6}$$

where $d^2(\mathbf{Q}_i)$ represents the contribuition of the undivided Laplacian operator, ans $d^4(\mathbf{Q}_i)$ the contribuition of the biharmonic operator. The biharmonic operator is responsible for providing the background dissipation to damp high frequency uncoupled error modes and the undivided Laplacian artificial dissipation operator prevents oscillations near shock waves. Thus, $d^2(\mathbf{Q}_i)$ and $d^4(\mathbf{Q}_i)$ are given by:

$$d^2(\mathbf{Q}_i) = \sum_{k=1}^{3} \frac{\varepsilon_{ik}^{(2)}}{2} \alpha_{ik}(\mathbf{Q}_k - \mathbf{Q}_i), \tag{7}$$

$$d^4(\mathbf{Q}_i) = \sum_{k=1}^{3} \frac{\varepsilon_{ik}^{(4)}}{2} \alpha_{ik}(\nabla^2 \mathbf{Q}_k - \nabla^2 \mathbf{Q}_i) \tag{8}$$

where

$$\nabla^2 \mathbf{Q}_i = \sum_{k=1}^{3} (\mathbf{Q}_k - \mathbf{Q}_i), \qquad \alpha_{ik} = (\frac{V_i}{\Delta t_i} + \frac{V_k}{\Delta t_k}), \tag{9}$$

with

$$\varepsilon_{ik}^{(2)} = K^{(2)} max(\nu_i, \nu_k), \tag{10}$$

$$\varepsilon_{ik}^{(4)} = max[0, (K^{(4)} - \varepsilon_{ik}^{(2)})], \tag{11}$$

$$\nu_i = \frac{\sum_{k=1}^{3} |p_k - p_i|}{\sum_{k=1}^{3} (p_k + p_i)} \tag{12}$$

where $K^{(2)}$ and $K^{(4)}$ are adjustable constant.

Therefore, the Euler equations after be fully discretized in space and the explicit addition of artificial dissipation terms, can be written as:

$$\frac{d}{dt}(V_i \mathbf{Q}_i) + C(\mathbf{Q}_i) - D(\mathbf{Q}_i) = 0 \tag{13}$$

where $C(\mathbf{Q}_i)$ represents convective operator, given by:

$$\int_{S_i} (\mathbf{E}dy - \mathbf{F}dx) \approx C(\mathbf{Q}_i) = \sum_{k=1}^{3} [\mathbf{E}(\mathbf{Q}_{ik})(y_{k2} - y_{k1}) - \mathbf{F}(\mathbf{Q}_{ik})(x_{k2} - x_{k1})], \tag{14}$$

where

$$\mathbf{Q}_{ik} = \frac{1}{2}(\mathbf{Q}_i + \mathbf{Q}_k), \tag{15}$$

and the (x_{k1}, y_{k1}) and (x_{k2}, y_{k2}) are vertices which define the interface between the volumes i and k.

The time-marching Euler solver developed by Oliveira (1993) was used. The unsteady Euler code is based on Jamenson's finite volume and Runge-Kutta time-marching using a second-order accurate, 5-stage, explicit, hybrid scheme. The 2-D Euler equations in integral form are discretized by a finite volume procedure in an unstructured mesh. This scheme, already including the necessary terms to account for changes in cell area due to mesh motion or deformation, can be written as:

$$\begin{aligned}
\mathbf{Q}_i^{(0)} &= \mathbf{Q}_i^{(n)} \\
\mathbf{Q}_i^{(1)} &= \tfrac{V_i^n}{V_i^{n+1}} \mathbf{Q}_i^{(0)} - \alpha_1 \tfrac{\Delta t}{V_i^{n+1}} [C(\mathbf{Q}_i^{(0)}) - D(\mathbf{Q}_i^{(0)})] \\
\mathbf{Q}_i^{(2)} &= \tfrac{V_i^n}{V_i^{n+1}} \mathbf{Q}_i^{(0)} - \alpha_2 \tfrac{\Delta t}{V_i^{n+1}} [C(\mathbf{Q}_i^{(1)}) - D(\mathbf{Q}_i^{(1)})] \\
\mathbf{Q}_i^{(3)} &= \tfrac{V_i^n}{V_i^{n+1}} \mathbf{Q}_i^{(0)} - \alpha_3 \tfrac{\Delta t}{V_i^{n+1}} [C(\mathbf{Q}_i^{(2)}) - D(\mathbf{Q}_i^{(1)})] \\
\mathbf{Q}_i^{(4)} &= \tfrac{V_i^n}{V_i^{n+1}} \mathbf{Q}_i^{(0)} - \alpha_4 \tfrac{\Delta t}{V_i^{n+1}} [C(\mathbf{Q}_i^{(3)}) - D(\mathbf{Q}_i^{(1)})] \\
\mathbf{Q}_i^{(5)} &= \tfrac{V_i^n}{V_i^{n+1}} \mathbf{Q}_i^{(0)} - \alpha_5 \tfrac{\Delta t}{V_i^{n+1}} [C(\mathbf{Q}_i^{(4)}) - D(\mathbf{Q}_i^{(1)})] \\
\mathbf{Q}_i^{(n+1)} &= \tfrac{V_i^n}{V_i^{n+1}} \mathbf{Q}_i^{(5)}
\end{aligned} \tag{16}$$

The values used for the α coefficients are:

$$\alpha_1 = \frac{1}{4}, \qquad \alpha_2 = \frac{1}{6}, \qquad \alpha_3 = \frac{3}{8}, \qquad \alpha_4 = \frac{1}{2}, \qquad \alpha_5 = 1. \tag{17}$$

3. TIME-MARCHING AEROELASTIC ANALYSIS

Consider a "typical two-degrees-of-freedom" (DOF) airfoil section as shown in Fig.1. The equations of motion of this aeroelastic system can be written in the form (Bisplinghoff et al., 1996):

$$m\ddot{w} - S_\alpha \ddot{\alpha} + K_w w = -L, \qquad -S_\alpha \ddot{w} + I_\alpha \ddot{\alpha} + K_\alpha w = M_{ea}. \tag{18}$$

where w and α are airfoil vertical displacement and pitch DOF, respectively, m is sectional mass, S_α is the static moment about elastic axis, K_w and K_α are translational and torsional stiffness about elastic axis, respectively. Here the left-hand-side terms represent a linear structural model approximation for the vertical displacement and pitch coordinates. The right-hand-side terms represent the aerodynamic loading terms, which are obtained from CFD code.

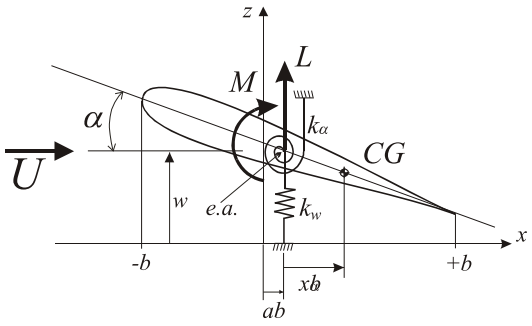

Figure 1. Typical section model.

In the current implementation, the same five-stage Runge-Kutta time-stepping scheme for the Euler equations is used for the aeroelastic equations. The aeroelastic solve is applied and incorporated within the CFD Euler code. The Runge-Kutta method needs the equations in terms of the state variables. Then, the system given by Eqs. (18) is adimensionalized and becomes:

$$\dot{q}_1 = q_2 \tag{19}$$

$$\dot{q}_2 = \frac{(U^*)^2(r_\alpha^2 C_L + 2x_\alpha C_m)}{(r_\alpha^2 - x_\alpha^2)\mu\pi} - \frac{r_\alpha^2\bar{\omega}^2 q_1 + r_\alpha^2 x_\alpha q_3}{(r_\alpha^2 - x_\alpha^2)} \tag{20}$$

$$\dot{q}_3 = q_4 \tag{21}$$

$$\dot{q}_4 = \frac{(U^*)^2(2C_m + x_\alpha C_L)}{(r_\alpha^2 - x_\alpha^2)\mu\pi} - \frac{\bar{\omega}^2 x_\alpha q_1 + r_\alpha^2 q_3}{(r_\alpha^2 - x_\alpha^2)} \tag{22}$$

with

$$q_1 = \frac{w}{b}; \qquad q_2 = \frac{\dot{w}}{b}; \qquad q_3 = \alpha; \qquad q_4 = \dot{\alpha}, \tag{23}$$

where b is semi-chord, μ is mass ratio, C_L and C_m are lift and pich moment coefficient, respectively, r_α is airfoil radius of gyration about elastic axis, x_α is nondimensional distance from elastic axis to mass center, $\bar{\omega} = \frac{\omega_w}{\omega_\alpha}$ where ω_w and ω_α are uncoupled natural frequency of bending and torsion modes, respectively, and the reduced velocity given by, $U^* = \frac{U_\infty}{b\omega_\alpha}$.

4. NON-LINEAR AEROELASTIC RESPONSES COMPUTATION

The results were calculated by first computing a converged steady flow solution about the airfoil, then forcing the airfoil in of 0.1 degree pitching about the elastic axis. The steady Euler solution was determined using the steady portion of the original unsteady Euler solver. The results of the steady Euler solution were validated by Oliveira (1993).

The subsequent aeroelastic response of the model was obtained by a time marching solution of the aeroelastic equations. The coupled computational fluid dynamic (CFD) and computational structural dynamics (CSD) method to the two-dimensional linear wing model as presented in the Section 3 was performed. This model simulates the bending and torsional motion of a wing cross section. It consists of two DOF, plunging and pitching, for a NACA0012 airfoil.

Time integration of the coupled fluid-structural equations of motion is obtained as follows:

1. At time level n, perform an iteration of the Euler equation and calculate values for C_L and C_m;
2. This information is sent to the structural equations, to determine the position and velocity of the airfoil;
3. The new position and velocity of the section are taken into account by the flow equations, and the process is repeated.

The solutions were determined on an unstructured mesh with 160 wall points and 11634 volumes that moved with the airfoil. To examine the effect of aerodynamic nonlinearities about the NACA0012 airfoil the following parameter were chosen:

$$x_\alpha = 1.8, \quad r_\alpha^2 = 3.48, \quad \bar{\omega} = 1, \quad \mu = 60, \quad a = -0.25. \tag{24}$$

Different Mach numbers and values of the reduced velocity, U^*, were considered for simulations. At a constant Mach number 0.9, a series of time integrations was performed at increasing reduced velocities. Figure 2 presents a simulation

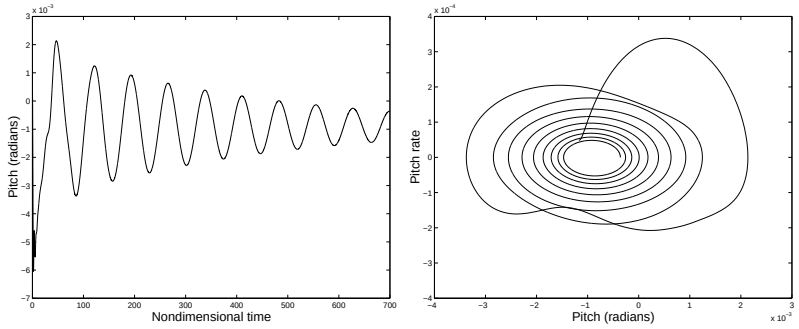

(a) (b)

Figure 2. (a) Time history (damped response). (b) Phase plane ($M = 0.9$, $U^* = 35$).

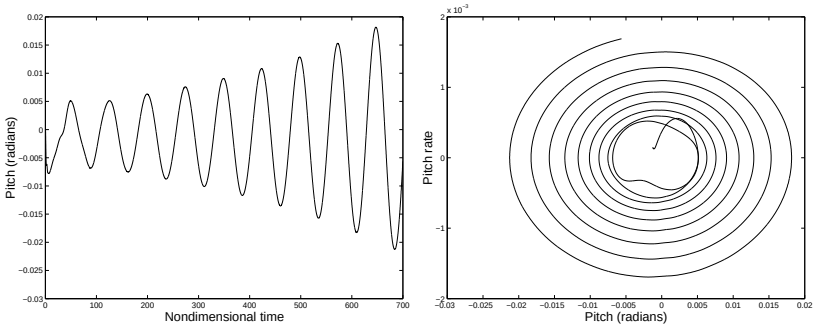

(a) (b)

Figure 3. (a) Time history (divergent response). (b) Phase plane ($M = 0.9$, $U^* = 45$).

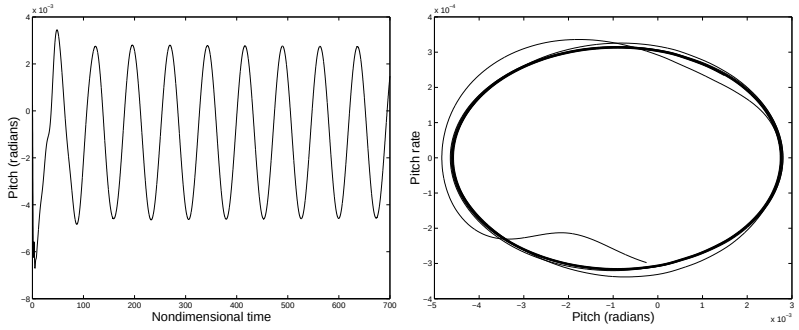

(a) (b)

Figure 4. (a) Time history. (b) Phase plane ($M = 0.9$, $U^* = 40$).

for $U^* = 35$, where the system approaches the stable equilibrium point between 0 and -1. Figure 3 shows divergent response system for $U^* = 45$, opposingly to the results in Fig. 2.

In between these two U^* conditions, there must be a particular point where the system is neutrally stable. This is shown in Fig. 4, when $U^* = 40$. However, most of the runs do not need computations for many time periods, because system oscillations were easily identified with diverging or converging amplitude by looking at only few of them.

For the present analysis, time integration for Mach number 0.85 were performed. Below a reduced velocity of $U^* = 35$, the system has presented an oscillatory mode with low amplitude. The results are shown in the Fig. 5, where it can be seen that the system first stabilizes in equilibrium point between 0 and -1 (*cf.* Fig. 5(a)) for $U^* = 10$ and limit cycle oscillations (*cf.* Fig. 5(b)) for $U^* = 23$. For reduced velocities above 23 to nearly 40, the system shows apparent divergent reponse as depicted in Fig. 6 for $U^* = 30$ and $U^* = 40$.

In Fig. 7, for $U^* = 50$, the system reaches a higher frequency oscillatory mode with slightly increasing amplitude.

For $U^* = 65$ (Fig. 8) shows the system initially diverging but then reaches a steady oscillatory mode with two slightly decreasing amplitudes. When $U^* = 70$ the system presented LCO with basically two amplitudes (*cf.* Fig. 9). For $U^* = 75$ the system has presented LCO behavior, but with varied amplitudes (*cf.* Fig. 10). In all cases, for $M = 0.85$, LCO amplitudes increase with the reduced velocity, where it seems to take the form of a supercritical bifurcation.

For reduced velocities above 80, the system experiences strong divergence conditions, with the results shown in Fig. 11. It can be noted, in comparison with the approach to limit cycles seen previously, that the divergence is extremely intense.

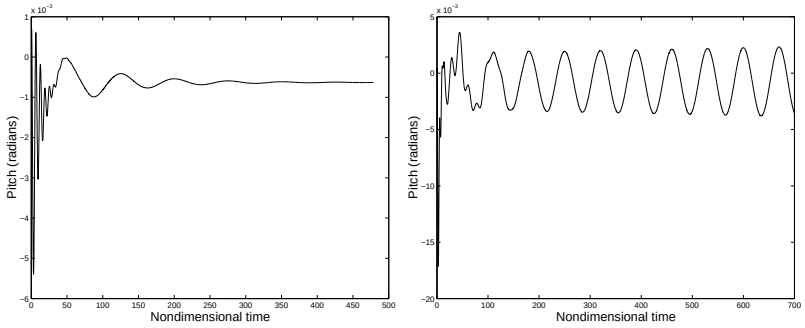

(a) (b)

Figure 5. (a) Time history, $M = 0.85$ and $U^* = 10$. (b) Time history, $M = 0.85$ and $U^* = 23$.

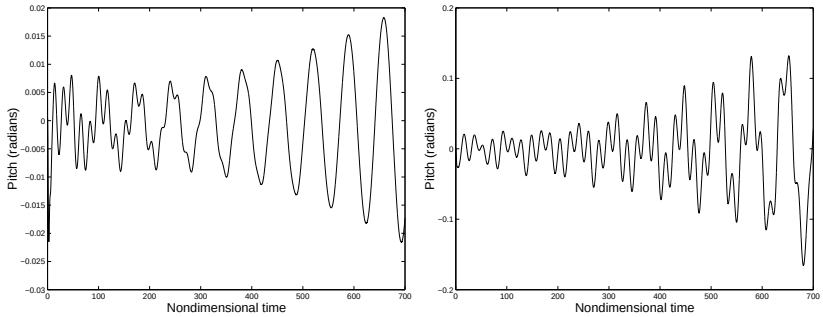

(a) (b)

Figure 6. (a) Time history, $M = 0.85$ and $U^* = 30$. (b) Time history, $M = 0.85$ and $U^* = 40$.

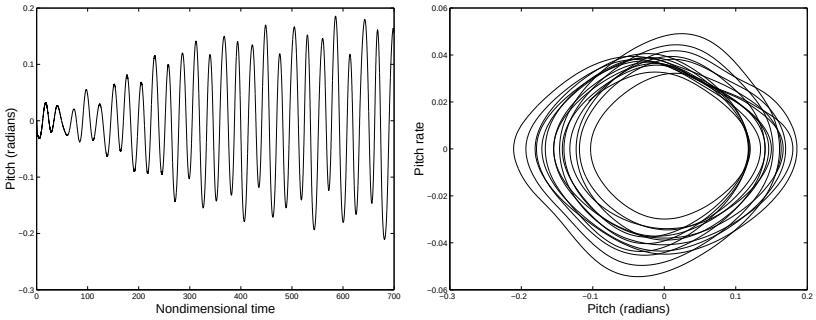

(a) (b)

Figure 7. (a) Time history (LCO). (b) Phase plane ($M = 0.85$, $U^* = 50$)

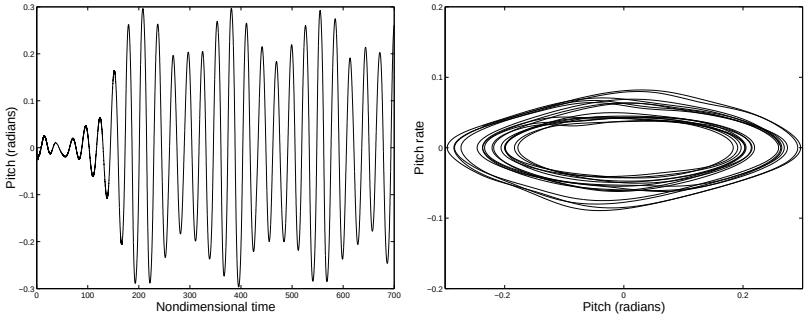

(a) (b)

Figure 8. (a) Time history (LCO). (b) Phase plane ($M = 0.85$, $U^* = 65$).

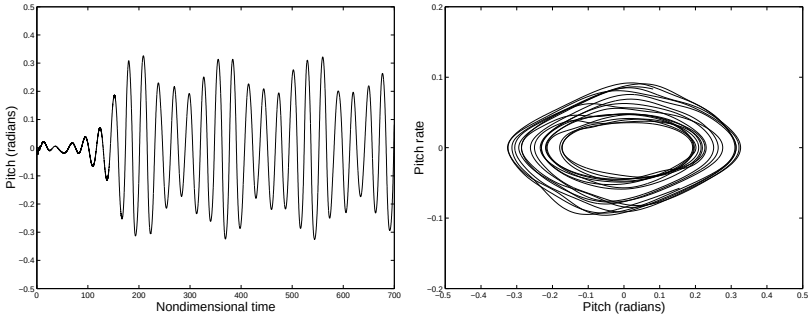

(a) (b)

Figure 9. (a) Time history (LCO). (b) Phase plane ($M = 0.85$, $U^* = 70$)

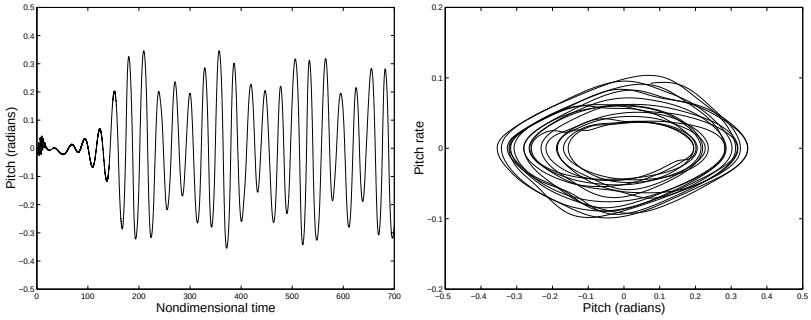

(a) (b)

Figure 10. (a) Time history (LCO). (b) Phase plane ($M = 0.85$, $U^* = 75$).

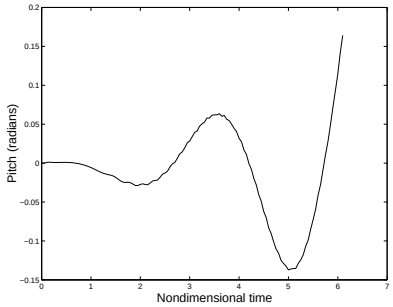

Figure 11. Strong divergence, $M = 0.85$ and $U^* = 80$.

5. CONCLUSIONS

A integrated fluid-structure simulation program has been developed for a simulation of nonlinear aeroelastic response behavior in transonic regime with linear structural parameters. This program consists of an aerodynamic models given by two-dimensional unsteady Euler solver and dynamic grid deformation code. To solve the aeroelastic problem the Runge-Kutta method is applied combined with the CFD code. The coupled CFD and structural method provides the time history of bending and torsional motion for a NACA0012 airfoil. The results has been analysed by time history and phase plane, where may be used to predict nonlinearities, although long computational time is needed for this porpose. For Mach number 0.85 the results have shown different modes and amplitude of oscillations, when reduced velocity increased from 10 to nearly 75, at which point a strong divergence condition is exceeded. These tests cases have presented the capability of the integrate CFD and structural program to predict LCO.

This analysis with Runge-Kutta methods for transonic aeroelastic system consist of primary analysis to predict nonlinear effects. Once validated, this work developements will provide bifurcations analysis for many flight conditions on transonic flow. Considering the effects of structural nonlinearities, it will advance to complete analysis of stability and bifurcation like LCO and chaos on transonic regime.

6. Acknowledgements

The authors would like to acknowledge the financial support from the Conselho Nacional de Desenvolvimento Científico e Tecnológico - CNPq and from the Fundação de Amparo à Pesquisa de Estado de São Paulo - FAPESP.

7. References

Alonso, J. J. and Jameson, A. 1994, "Fully-Implicit Time-Marching Aeroelastic Solutions", 32nd AIAA, Aerospace Sciences Meeting Exhibit, 32 nd, Reno, NV, 10-13 January.

Bunton, R. W. and Denegri, C. M., 2000," Limit Cycle Oscillation Characteristics of Flighter Aircraft", Journal of Aircraft, vol. 37, n. 5, pp. 916-918.

Cooper, J. E., 2003, "Towards Efficient Prediction of Nonlinear Aeroelastic Phenomena", Proceedings of the X DINAME, Ubatuba-SP-Brasil, pp. 289-296.

Denegri, C. M., Jr., 2000, "Limit Cycle Oscillation Flight Test Results of a Flighter with External Stores", Journal of Aircraft, vol. 37, n.5, pp. 761-769

Dowell, E. H. and Tang, D., 2002, "Nonlinear Aeroelasticity and Unsteady Aerodynamics", AIAA Journal, vol. 40, n. 9, pp. 1697-1707.

Dowell, E. H. and Tang, D. and Strganac, T. W., 2003, "Nonlinear Aeroelasticity", Journal of Aircraft, Vol. 40, n. 5, pp. 857-874.

Jameson, A. and Schmidt, W. & Turkel,E., 1981, "Numerical Simulation of the Euler Equation by Finite Volume Using Runge-Kutta Time Stepping Schemes", AIAA Paper, pp. 81-1259.

Kholodar, D. B. K. and Thomas, J. P. and Dowell, E. H. and Hall,K. C., 2003 "Parametric Study of Flutter for an Airfoil in Inviscid Transonic Flow", Journal of Aircraft, vol. 40, n. 2, pp. 303-313, Mar-Apr.

Kousen, K. A. and Bendiksen, O. O., 1994, "Limit Cycle Phenomena in Computational Transonic Aeroelasticity", Journal of aircraft, vo. 32, n. 2, pp. 1257-1263.

Lee, B. H. K. and Price, S. J. and Wong, Y. S., 1999, "Nonlinear Aeroelastic Analysis of Airfoils: Bifurcation and Chaos", Progress in Aerospace Sciences, Vol.35, pp. 205-334.

Liu, F. and Cai, J. and Zhu, Y. and Tsai, H. M. and Wong, A. S. F., 2001, "Calculation of Wing Flutter by a Coupled Fluid-Structure Method", Journal of Aircraft, vol. 38, n. 2, pp. 334-342, Mar-Apr.

Oliveira, L. C., 1993, "A State-Space Aeroelastic Analysis Methodology Using Computational Aerodynamics Techniques", Master Thesis - Instituto Tecnológico de Aeronáutica, São José dos Campos, S. P., Brazil. (in Portuguese, original title is "Uma Metodologia de Análise Aeroelástica com Variáveis de Estado Utilizando Técnicas de Aerodinâmica Computacional").

Thomas, J. P. and Dowell, E. H. and Hall, K. C., 2002, "Nonlinear Inviscid Aerodynamic Effects on Transonic Divergence, Flutter, and Limit-Cycle Oscillations", AIAA Journal, vol. 40, n. 4, pp. 638-646.

8. Responsibility notice

The authors are the only responsible for the printed material included in this paper.